Materials Research Proceedings 28 (2023) 2037-2048 https://doi.org/10.21741/9781644902479-219

Cryogenic reverse flow forming of AISI 304L

ARIAN Bahman[1,a *], HOMBERG Werner[1,b], ROZO VASQUEZ Julian[2,c], WALTHER Frank[2,d], KERSTING Lukas[3,e] and TRÄCHTLER Ansgar[3,f]

[1]Paderborn University, Forming and Machining Technology (LUF), Germany

[2]TU Dortmund University, Chair of Materials Test Engineering (WPT), Germany

[3]Fraunhofer Institute for Mechatronic Systems Design (IEM), Germany

[a]ba@luf.upb.de, [b]wh@luf.upb.de,[c]julian.rozo@tu-dortmund.de, [d]frank.walther@tu-dortmund.de, [e]lukas.kersting@iem.fraunhofer.de, [f]Ansgar.Traechtler@hni.uni-paderborn.de

Keywords: Reverse Flow Forming, Cryo Forming, α'-Martensite, Closed-Loop Control

Abstract. Workpiece property-control permits the application-oriented and time-efficient production of components. In reverse flow forming, for example, a control of the microstructure profile is not yet part of the state of the art, in contrast to the geometry control. This is, due to several reasons, particularly challenging when forming seamless tubes made of metastable austenitic stainless AISI 304L steel. Inducing mechanical and/or thermal energy can cause a phase transformation from austenite to martensite within this steel. The resulting α'-martensite has different mechanical and micromagnetic properties, which can be advantageous depending on the application. For purposes of local property control, the resulting α'-martensite content should be measured and controlled online during the forming process. This paper presents results from the usage of a custom developed cryo-system and different application strategies to use liquid nitrogen as a coolant for local enhancement of the forming-temperature depending α'-martensite content.

Introduction

With growing customer demands the requirements on materials, tools and processes within manufacturing companies are increasing accordingly [1]. Therefore, one of the main objectives of production and manufacturing technology is the reproducible production of (complex) defect-free components. The control of local workpiece properties (e.g. microstructure profile), satisfying customer needs while meeting requirements, has gained more and more importance. This still constitutes a challenge in reverse flow forming, since the process is affected by a large number of influencing factors e.g. tool and machine behavior, properties of the semi-finished product like eccentricity as well as the chemical composition and is therefore hard to predict [2]. A promising approach in this context is an according closed-loop process control. Extensive experimental investigations were carried out in regard to a better control of the α'-martensite content in austenitic stainless steel (AISI 304L) tubes during thermomechanical reverse flow forming. The focus of the investigations was the use of temperature as a control variable to influence local transformation behavior. Since cooling favors the phase transformation (austenite → α'-martensite) liquid nitrogen was applied through a custom developed cryogenic nozzle to maximize the cooling effect and therefore the α'-martensite formation. As part of the cryogenic reverse flow forming different process strategies (timing of cooling during the process) and different cooling strategies (varying cooling areas to produce axial and axial-angular graded α'-martensite areas) were investigated. Local property control e.g. wall thickness and α'-martensite offers an advantage in product labeling. This method can be utilized for a unique, invisible and novel product identification comparable to an invisible QR code. The local manipulation of the α'-martensite content, while maintaining the external dimensions, generates an individual and invisible microstructure profile, making the products tamper-proof. Previous and current work has shown, that two strategies can

be differentiated to decouple the geometry and the product properties. The first strategy employs a multi-stage process that utilizes process parameters such as the feed rate and infeed, which has been demonstrated to be effective in earlier research. Our previous investigations have shown a correlation between the selection of these parameters and the α'-martensite content, while maintaining the external dimensions [3]. The second strategy is part of current work and involves thermomechanical forming, which locally affects the formation of α'-martensite in a single-stage process through the active manipulation of temperature (cooling/heating). To locally grade properties such as the α'-martensite content, it is necessary to differentiate between grading directions. One approach to improve the properties of the tube is through axial grading, where the martensite content is varied along the length of the tube. While previous research has shown success in this method [3], current efforts aim to enhance the technique by also controlling the α'-martensite content in the angular/circumferential direction. For this, rapid cooling methods or periodic/cyclic local cooling or heating must be implemented during the tube forming process, as the tubes need to reach varying temperature profiles in both the length and angular direction as they rotate. However, precise control of these properties remains a challenge and is yet to be established as a common practice. The ongoing research endeavors to develop new techniques and methods to overcome these challenges and achieve the desired level of local property control. The α'-martensite contents for local grading of the microstructure profile and the creation of an invisible labeling of the components must be distinctly detectable for the sensors to be used. The differences of the martensitic and non-martensitic ranges must be well above the measurement uncertainty of the measuring instrument. For these investigations the feritscope FMP30 from Helmut Fischer was used with a measuring accuracy of approx. ±1 %.

Principles and Material

Flow forming as an incremental process offers various advantages in terms of flexibility and efficiency [4]. Based on a defined wall thickness reduction within tubular components the process allows the production of parts with an excellent shape and dimensional accuracy as well as prime surface qualities [5]. Components that meet such high standards and offer the above-mentioned advantages can be used to produce, among others, components for the aerospace industry. Here, precision and lightweight play an essential role, which is covered by flow forming. Just to name a few application examples: drive shafts for jet engines and helicopters are flow formed components [6]. In principle, the rotating tube is set backlash-free on a rotating mandrel and is typically deformed by a multiple roller tool arrangement generating the necessary deformation forces for the wall thickness reduction. The roller tools can be moved in radial and axial direction, reducing the outer diameter of the tube and thus generating an elongation. In reverse flow forming, the material flows in the opposite direction to the roller tool movement [7], as demonstrated in Fig. 1. This process is the focus of this paper.

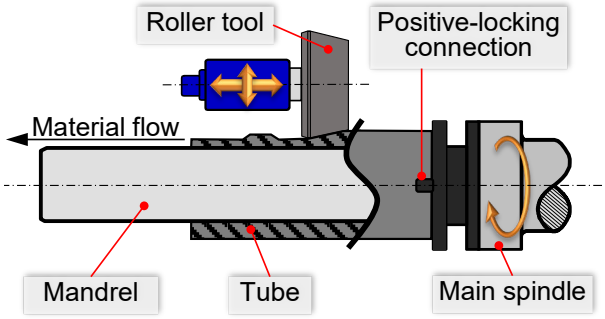

Fig. 1. Reverse flow forming principle.

The stainless steel AISI 304L (X2CrNi18-9, 1.4307), which is used as semi-finished material for the seamless tubes, is austenitic. Containing a metastable austenitic phase, a phase transformation from austenite to α'-martensite could occur strain- or temperature-induced [8]. The α'-martensite, nucleating at the intersections of the shear bands, has different mechanical and micromagnetic properties and can be detected offline (e.g. Feritscope) or online via micromagnetic sensor equipment (e.g. 3MA-II) like addressed in previous papers [9,10,11]. Besides the mentioned influencing factors, the α'-martensite formation is also dependent of the chemical composition and the austenite grain size of the semi-finished product [12,13]. Depending on the chemical composition of the material batch the potential for α'-martensite formation can significantly vary. The used material batch offers a qualitatively low potential for α'-martensite formation, since fractions of austenite stabilizing elements like nickel are relatively high [14]. Comparisons with different material batches show for the same process parameter combinations variations in resulting α'-martensite content between approx. 10 % and 85 %. This aspect again emphasizes the need for property control. For material batches with low potential for α'-martensite formation, more deformation and/or lower (cryogenic) forming temperatures must be achieved to reach similar α'-martensite contents. Since the semi-finished tubes with an outer diameter of 80 mm are seamless, they contain an eccentricity and therefore slight deviations from the nominal wall thickness of 4 mm.

Machine and Experimental Setup

All experiments were carried out on a PLB 400 spinning machine from Leifeld Metal Spinning GmbH (Ahlen, Germany) with a drive power of 11 kW and a maximum achievable spindle speed of 950 rpm. The hydraulically driven cross support equipped with two machining axes, was developed at LUF at Paderborn University and is capable of generating a maximum force of 35 kN on each of its axes (X/Y-axis). By default, the operating pressure of the external hydraulic system amounts 80 bar and can be increased up to 120 bar, when required. Additionally, a universal tool holder allows the attachment of a variety of tools or tool systems. For the investigations, a single-roller tool configuration was used to provide enough space for the sensor equipment, which will be applied for online-measurement purposes, which was presented in previous publications of the authors and is not the focus of this paper. The roller has an attack angle of $\alpha = 12°$, a transition radius of $R = 2$ mm and an exit angle of $\beta = 5°$. For the external dimensions, a rolling diameter of 155 mm and a roller width of 46.5 mm can be measured. In the process, a solid counter holder with two ball-bearing counter rollers is used to support the mandrel. A cryogenic cooling system was developed for the experiments and placed on the machine bed. It contains a liquid nitrogen tank, a flexible stainless steel tube for the liquid nitrogen, pneumatic tubes, a set of valves and a two-component cryogenic nozzle that bundles the liquid nitrogen and transports it with compressed air surrounding it. The cryogenic nozzle was mounted in a distance of 8 mm from the specimen, which was to be deformed. For temperature monitoring an infrared camera (Infratech VarioCam head HiRes 640) was used. Fig. 2 shows the machine and experimental setup.

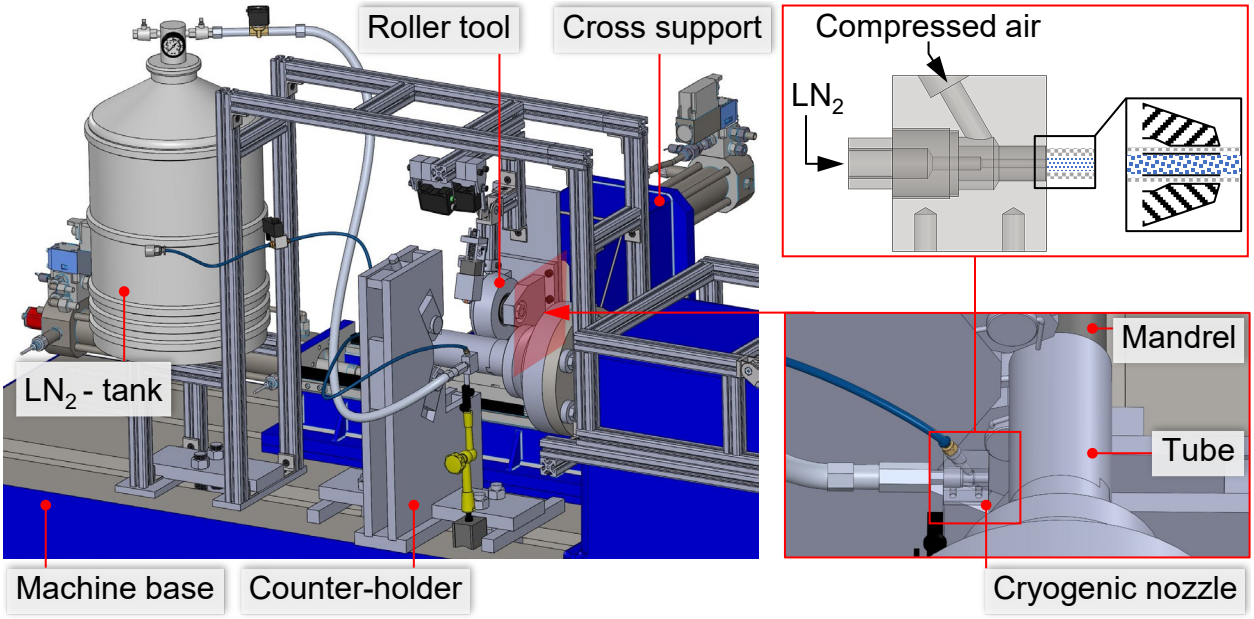

Fig. 2. Machine and experimental setup as 3D-model.

Experiments with three different cooling strategies were conducted. In the first experimental cooling strategy, the tube was rotated and simultaneously shock-cooled for a certain period of time prior to forming. Due to the stationary positioning of the cryogenic nozzle, this resulted in an axial section on the tube which was cooled down circumferentially (ring-shaped cooling prior to forming). The second experimental set-up was performed in analogy to the first strategy, with the difference that the shock cooling was conducted simultaneously to the flow forming (ring-shaped cooling while forming). In the third experimental set-up the aim was to create a spot that was shock-cooled before forming, which is why the rotation was switched off during the cooling of the component. (spot cooling prior to forming). For all three cooling strategies a radial infeed of 2 mm, a feed rate of 0.1 mm/s and a rotational speed of 5 rpm was selected. Fig. 3 shows the initial state of the specimens and the deformed specimens on which the cooled areas are highlighted in red.

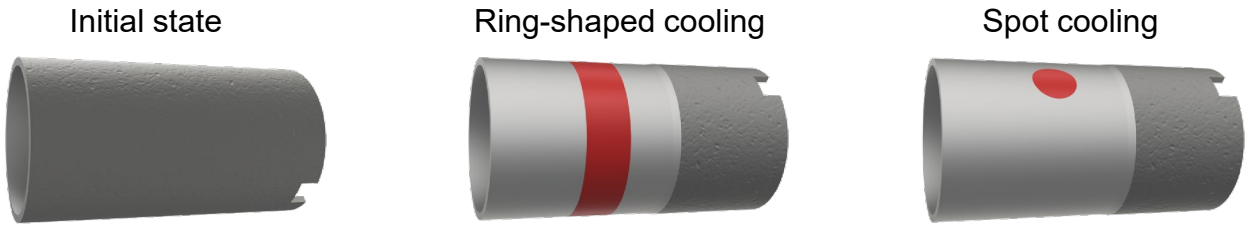

Fig. 3. Cryogenic deformed areas on specimens (highlighted in red).

Results and Discussion

For the first cooling strategy (ring-shaped cooling prior to forming) the tube, with an initial temperature of 16°C, was cooled down with the liquid nitrogen in the ring-shaped area for approx. 200 s to -8°C using a rotational speed of 5 rpm. Then the reverse flow forming process was initiated. The time span between the cooling of the tube and the deformation of the ring-shaped cooled area was approx. 115 s and the initial pressure of the liquid nitrogen tank was at 0.5 bar.

For the second cooling strategy (ring-shaped cooling while forming) the tube had an initial temperature of 17°C and was also cooled down to -8°C in the ring-shaped area using the liquid nitrogen. In this case, the forming process was started before cooling. Only after reaching the tube section to be cooled, the cooling was started and sustained for approx. 200 s, also at an initial

pressure of 0.5 bar. At a feed rate of 0.1 mm/s, an axial tube section of 20 mm was thus formed with active cooling. Fig. 4 shows the actual setup for the second cooling strategy.

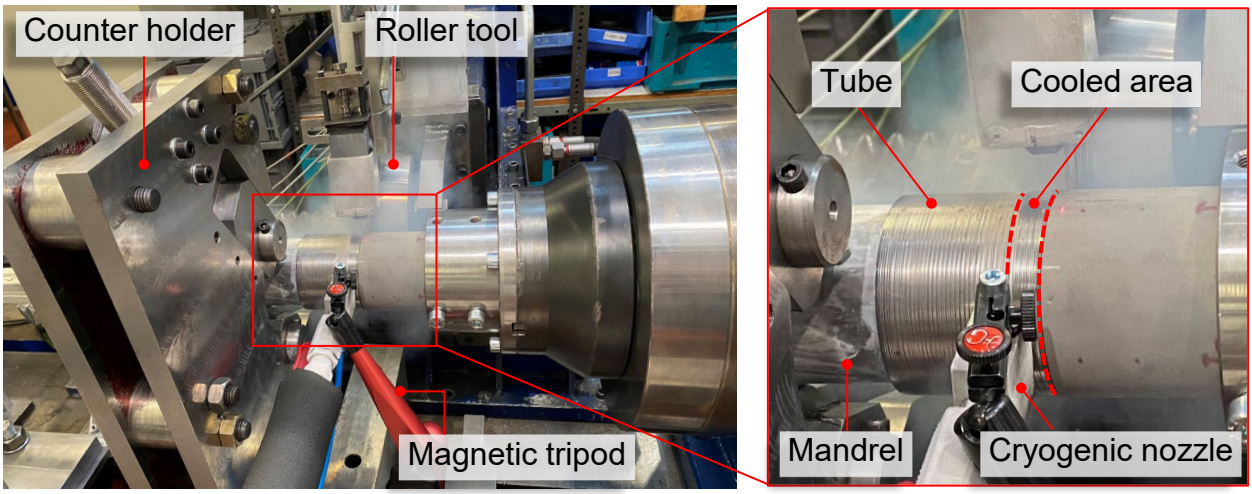

Fig. 4. Ring-shaped cooling while forming (second cooling strategy).

The third cooling strategy (spot cooling prior to forming) included a tube with an initial temperature of 15°C. After the reverse flow forming process was initiated prior to cooling, the axial feed and the rotation of the mandrel was switched off while forming was taking place. The system was switched off so that the area, in this case a circular spot, could be cooled down for approx. 130 s until the surface of the tube was frozen, again with a liquid nitrogen tank pressure of 0.5 bar. The infrared camera was not able to measure the temperature in the spot since it displayed a temperature of -273.15°C, which corresponds to absolute zero with 0 K. Then the cooling process was stopped and the reverse flow forming process was restarted to form the cooled spot as well as the rest of the tube. Here, the cooling process was not sustained while forming, since the rotation would again result in the cooling of a ring-shaped area. Fig. 5 shows the actual setup for the cooling strategy.

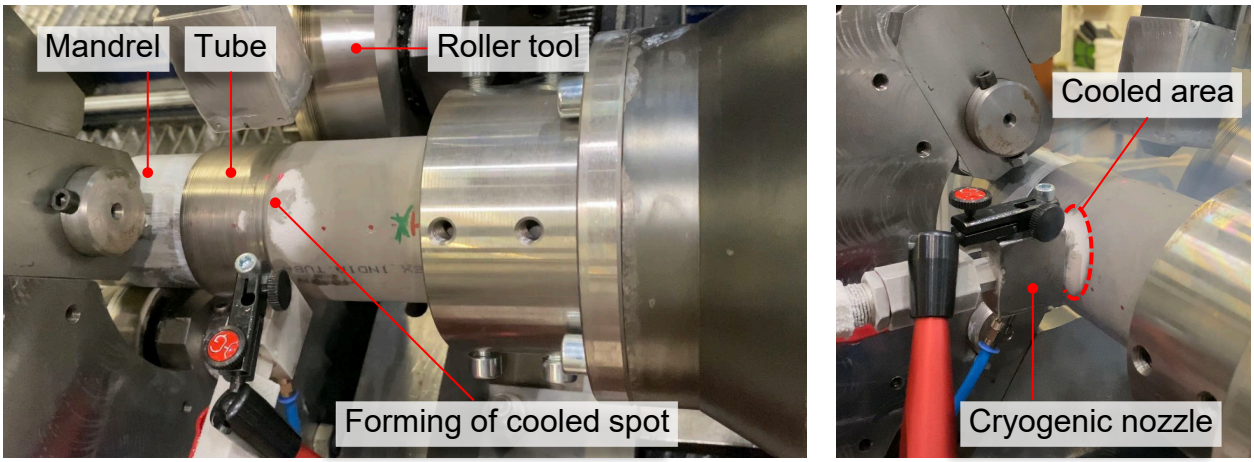

Fig. 5. Spot cooling prior to forming (experiment 3).

The resulting tubes were investigated through measurements with a Feritscope (FMP 30, Helmut Fischer) using the magnetic induction method, a micromagnetic sensor (3MA-II, Fraunhofer IZFP) based on magnetic Barkhausen noise (MBN) effect, eddy current analysis (Modulus r - 200 kHz) and hardness tests (HV3). The measurements were used to localize and

quantify the α'-martensite content, which correlates with the underlying measured variables such as the maximum amplitude of the MBN profile (Mmax) [15,16]. Fig. 6 shows the measurement results with the Feritscope, where cooled areas show higher α'-martensite contents. Four measuring circles with identical distances of 22 mm were used for the measurements. For this purpose, the measuring circles were divided into 30°-sections. The result for the second cooling strategy shows the highest α'-martensite content with a maximum of approx. 17 vol.-%, which is comparatively low due to the chemical composition of this specific material batch, which contains high proportions of austenite-stabilizing elements. This result can also be explained by the fact that the component was deformed during cooling and therefore could not warm up towards room temperature before deformation, in contrast to the first cooling strategy. Also, the coolant flow continuously dissipates the forming heat. In addition to measuring circle 2 where the cooling was mainly carried out, an increased α'-martensite content can be observed in measuring circle 1. This is due to the fact that this section adjacent to measuring circle 2 was also cooled during the cooling of measuring circle 2. Since there is little time between the cooling of measuring circle 2 and the forming of measuring circle 1, this result is also reasonable. The ups and downs for the α'-martensite measurement in the measuring circle 2 are due to pulsation of the liquid nitrogen. As a result of the evaporation of the liquid nitrogen, due to the comparatively warm hose, liquid nitrogen and a gas mixture alternately escape from the nozzle. This leads to inhomogeneous cooling of the rotating tube section. The first cooling strategy shows the same effect due to pulsation of the liquid nitrogen. The α'-martensite content is also lower than for cooling strategy 2, which is due to the time span between the cooling of and the deformation of the ring-shaped cooled area. For the cooling strategy 3 only one large peak for the α'-martensite content is visible, since only one spot was cooled down. An increase in α'-martensite content for areas close to the spot is due to thermal conduction to the adjacent area.

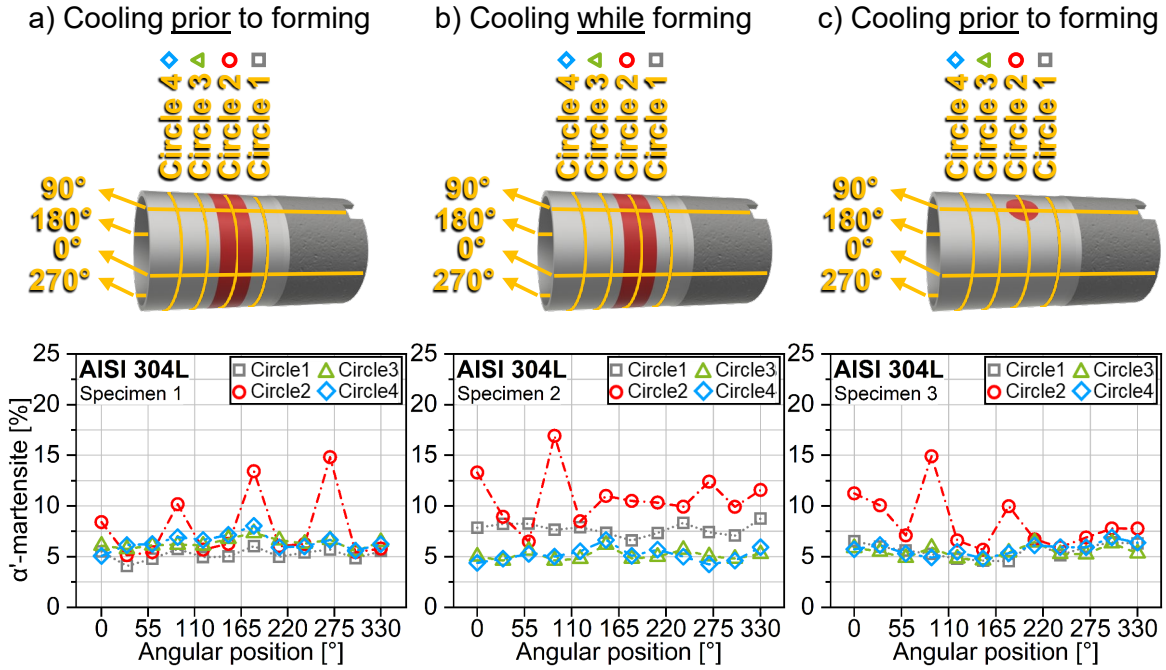

Fig. 6. Feritscope measurement results for the three applied cooling strategies.

The measurements with magnetic Barkhausen noise (MBN) effect performed with the 3MA-II, shown in Fig. 7, also display higher values for measuring circle 2, which is located in the cooled areas. Similar to the previous measurements with the Feritscope, areas adjacent to measuring circle 2 also have slightly higher values, as they have been co-cooled.

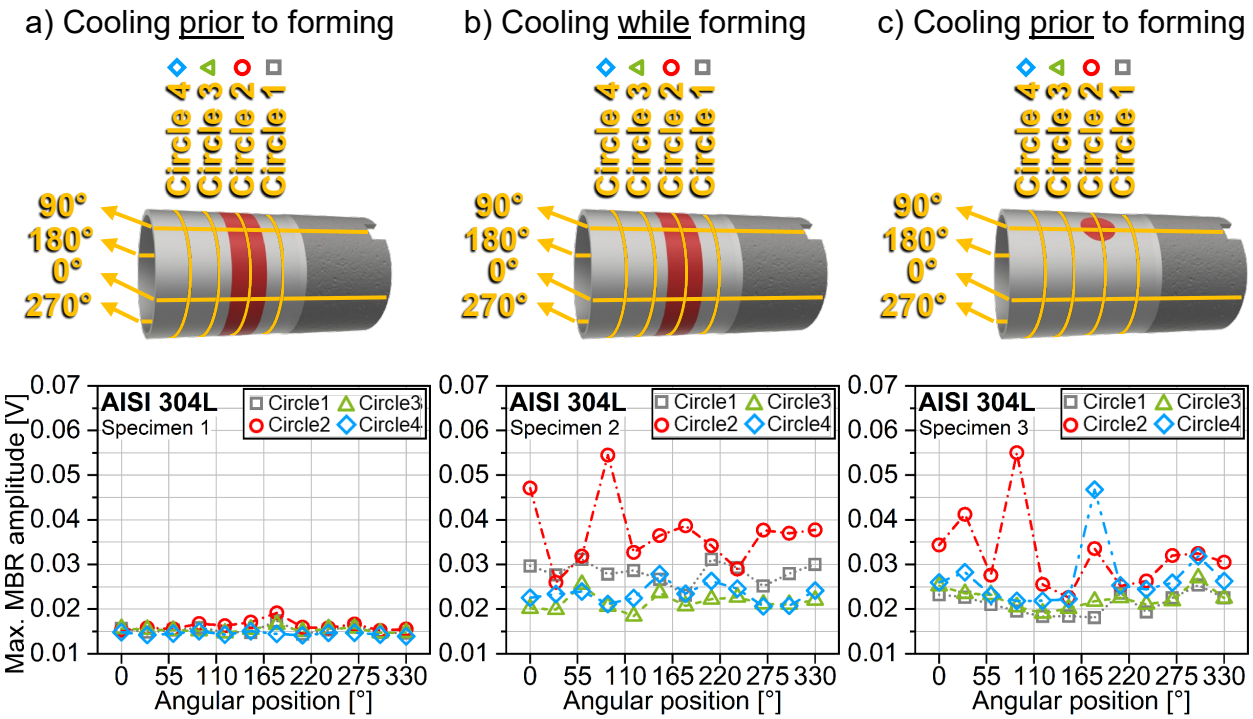

Fig. 7. 3MA-II measurement results for the three applied cooling strategies.

Other than expected, here the values for the measurements regarding cooling strategy 1 show low magnitudes for measuring circle 2. This might be due to the fact that the areas with martensitic microstructure might be smaller in terms of area than in cooling strategy 2, for example. However, it may also be caused by disturbance influences such as the incorrect alignment of the measuring head to the workpiece.

Eddy current analysis was used as a further non-destructive characterization technique. The changes of conductivity and permeability of the material due to the phase transformation from austenite into α'-martensite can be detected by means of the parameter "modulus r". This parameter is computed from real and imaginary parts of the impedance vector corresponding to each deformation state with respect to a point considered as the initial condition (unformed metastable austenite). The measurements, shown in Fig. 8, indicate a strong similarity to the measurements with the Feritscope. Here, the correlation of the measuring variable with the α'-martensite is also visible. The comparison of the measured α'-martensite contents with the Feritscope in Fig. 6 shows in cooling strategy 1 there are higher magnitudes for the parameter "modulus r" for lower α'-martensite contents, which could be due to a superposition of effects triggered by other variables influencing "modulus r".

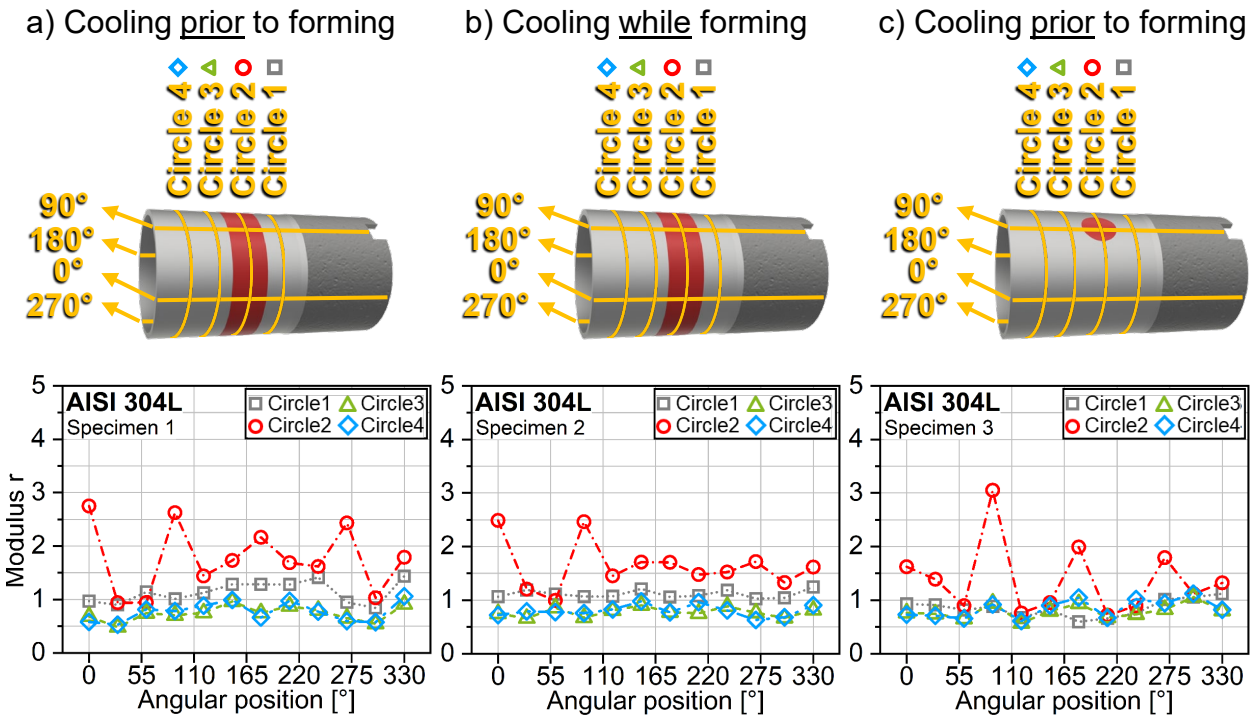

Fig. 8. Eddy current analysis for the three applied cooling strategies.

A comparison of the results from the hardness tests (HV3) in Fig. 9 show the same correlation with the α'-martensite content. The hardness increases with higher magnitudes of α'-martensite. As can be seen, for example, from the measurements for cooling strategy 3, the highest value for hardness results here, although the α'-martensite content is higher for cooling strategy 2 (compare Fig. 6). This is due to the influence by the work hardening, which can be quite different.

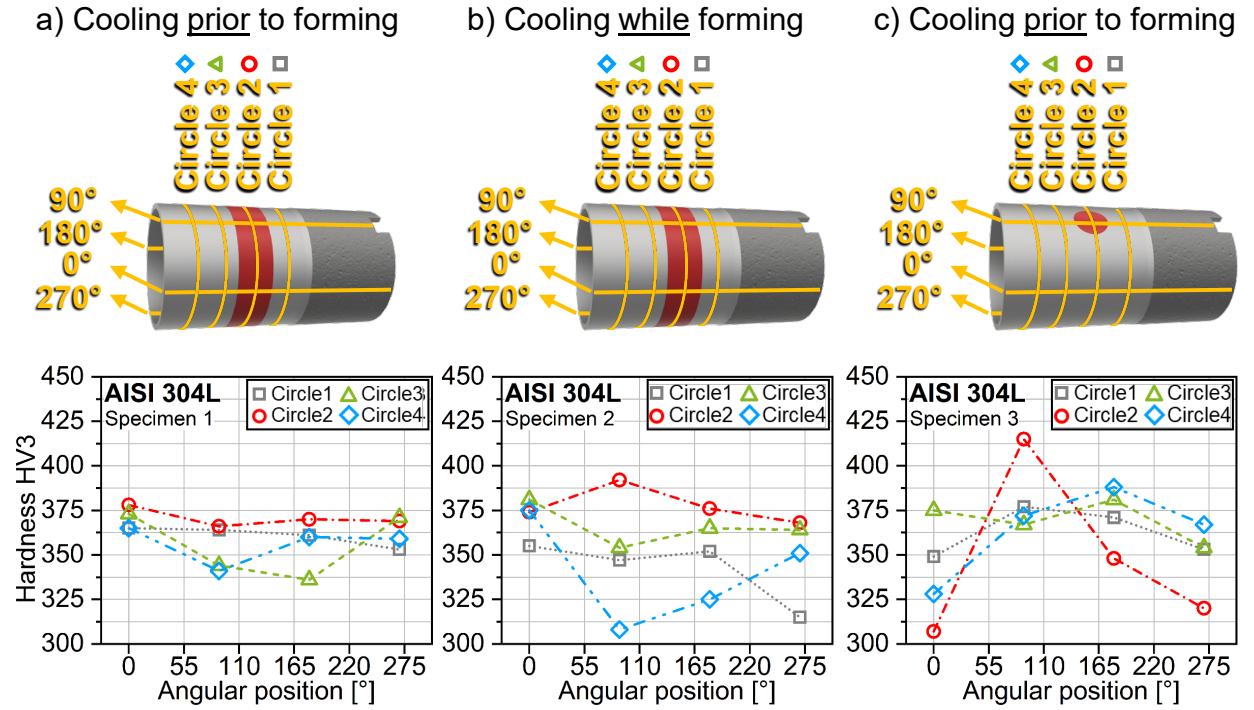

Fig. 9. Hardness tests (HV3) for the three applied cooling strategies.

Investigations of the wall thickness (compare Fig. 10) did not show any influence caused by the martensitic microstructure. The wall thickness increase in feed direction of the roller tool is caused due to material-pile-up in feed direction.

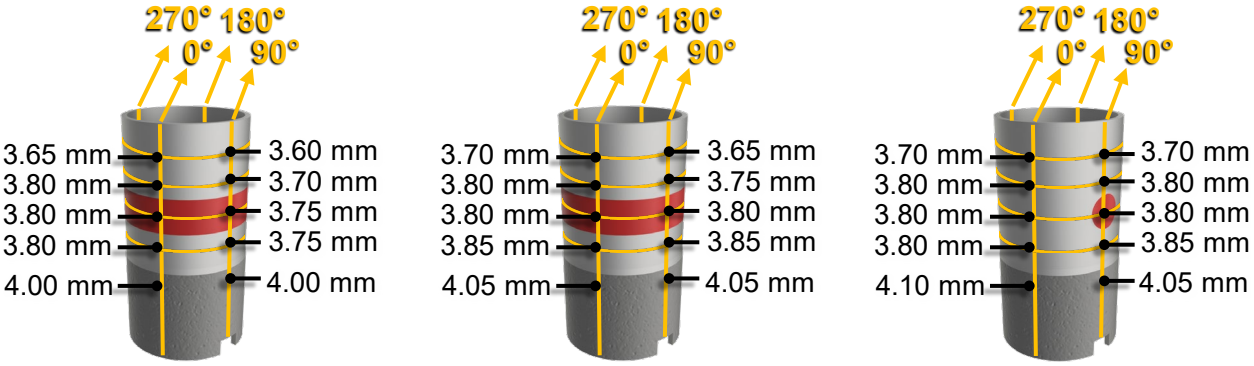

Fig. 10. Wall thicknesses resulting from the three applied cooling strategies.

The EBSD results in Fig. 11 show the microstructure of the cryogenic flow formed areas. The phase mappings display a qualitative distribution of austenite (blue) and α'-martensite (red) phases. The inverse pole figure (IPF) shows the grain orientation of the microstructure. The pictures of the areas deformed at room temperature conditions, indicate almost no transformation of the microstructure, which remains predominantly austenite (blue color in the phase mapping). This correlates well with the micromagnetic measurements on these areas, where almost no α'-martensite was detected. On the cryogenic flow formed area the dark lines in both pictures correspond to shear bands, which are a characteristic of the phase transformation during plastic deformation of metastable austenite. The intersection points of these shear bands are energetically favored nucleation points of the α'-martensite (red color in the phase mapping), which is shown on the red colored areas of the phase mapping.

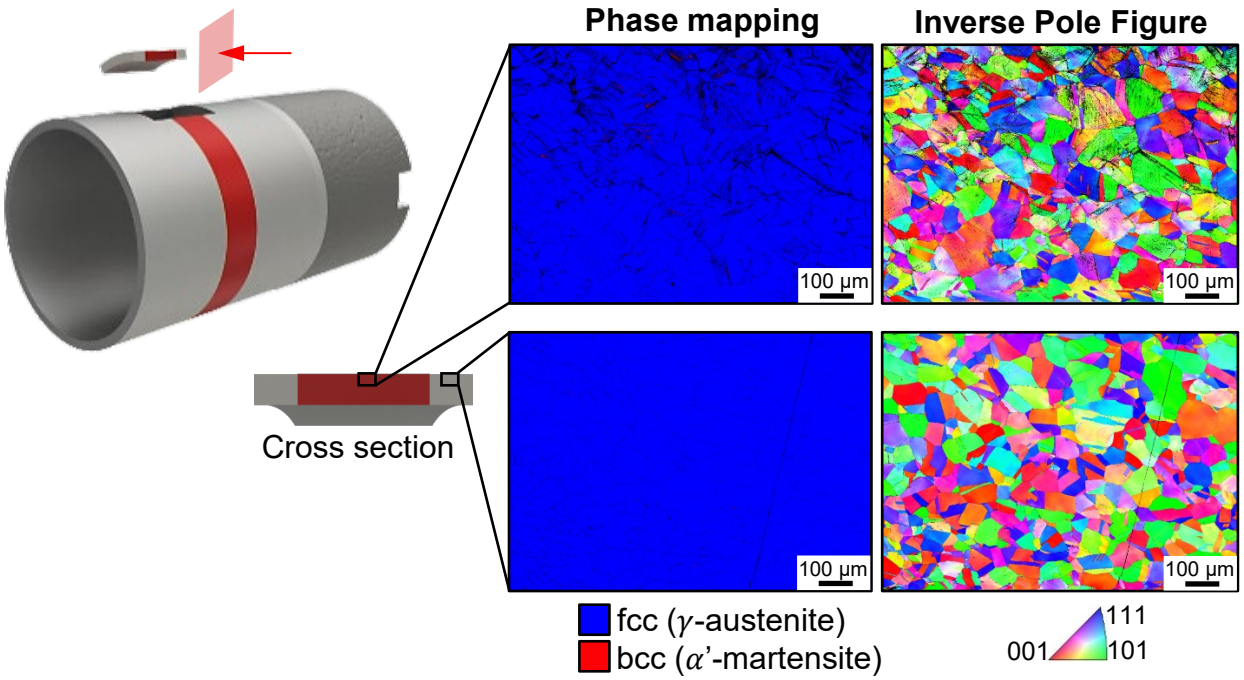

Fig. 11. EBSD results of the microstructure of the cryogenic flow formed area: phase mapping and inverse pole figure (IPF).

A higher quantity of shear bands and nucleation points of α'-martensite is present close to the outer surface, where the cryogenic deformation occurs. On the deeper areas, the deformation decreases which is evidenced in a lower quantity of shear bands and α'-martensite.

Summary

The results from the investigation show that the cryo system is useful for the invisible local enhancement of the α'-martensite content. The cryogenic nozzle is capable of focusing the liquid nitrogen surrounded by compressed air to form a cooling jet. As a result from the investigation of the different cooling strategies, cooling during forming was found to be the most effective method for maximizing the α'-martensite content. The investigations also show that the material batch of the tube used allows comparatively little α'-martensite formation due to its chemical composition, which contains high proportions of austenite-stabilizing elements. The investigations have also shown that automation of the cooling, i.e. inclusion of the cooling strategy in the process control, appears to be useful. Currently, to cool a spot, as with cooling strategy 3, both process stop and shock cooling were performed manually. In the future, the cryogenic system is to be further developed so that position-dependent (depending on the axial position of the roller tool) and angle-dependent (angular position of the tube to be formed) cooling is controlled automatically. This enables the automated production of so-called 2D-gradations (axially and angularly graded structures) similar to cooling strategy 3. For this purpose, an absolute encoder has been implemented within the forming machine, via which the angular position of the tube can also be incorporated into the control system. Furthermore, electromagnetic valves are currently being implemented in the control system in order to automate the release of the liquid nitrogen and the compressed air. The planned design of the cryogenic system is shown in Fig. 12.

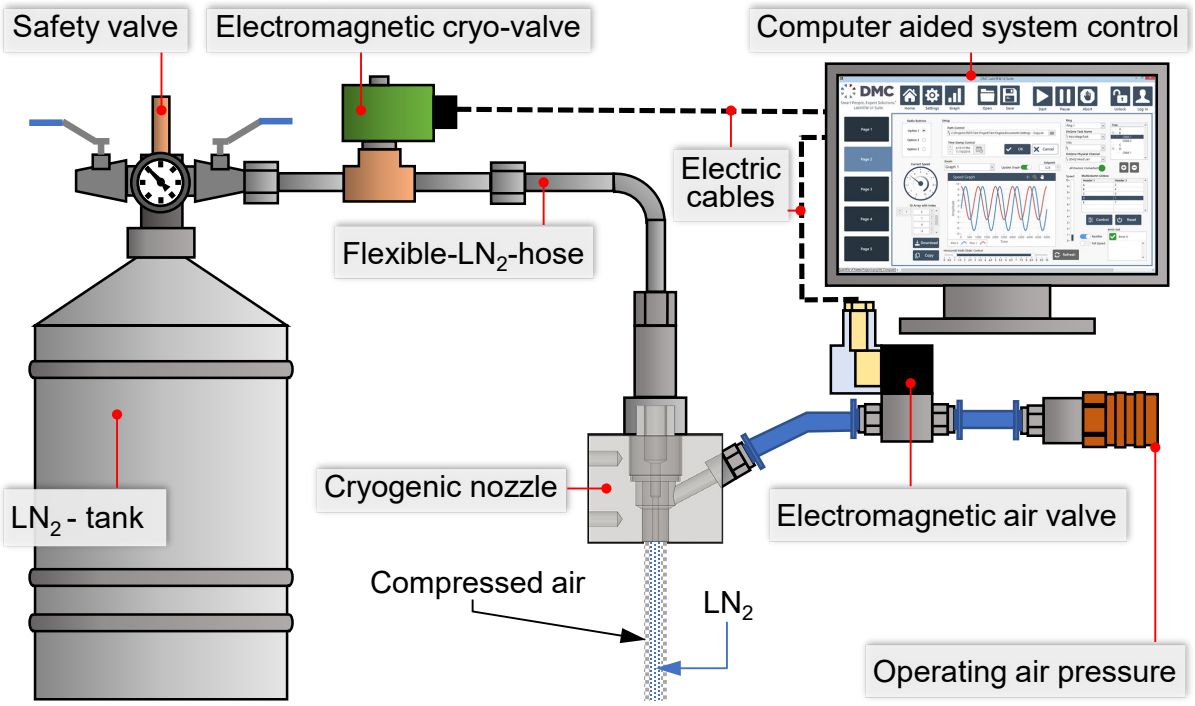

Fig. 12. Planned cryogenic system design.

With regard to thermomechanical forming, ongoing work is currently being conducted on an induction system which is to be used for purposely lowering the α'-martensite content locally through heating. In this way, for example, the co-cooling of adjacent tube sections can be prevented, which can improve the grading sharpness in the axial and angular direction. The

sharpness of local gradients in the grading process depends on various factors, including the geometry of the roller tool determining the contact area (e.g. transition radius and the attack angle of the roller), the achievable temperature differences in the areas being formed, the thermal conductivity of the material, the duration between cooling and forming. These factors, along with the constraints of the forming machine, such as achievable process parameters and actor dynamic, affect the formation of α' martensite and the distinction between different areas. Contact with warm tools and resulting process heat can decrease the temperature differences crucial for grading sharpness. These aspects are currently being investigated and will be quantified in future work.

Acknowledgment
The authors would like to thank the German Research Foundation (Deutsche Forschungsgemeinschaft, DFG) for their support of the depicted research within the priority program SPP 2183 "Property controlled deformation processes", through project no. 424335026 "Property control during spinning of metastable austenites". The authors further thank the German Research Foundation and the Ministry of Culture and Science of North Rhine-Westphalia (Ministerium für Kultur und Wissenschaft des Landes Nordrhein-Westfalen, MKWNRW) for funding of the Focused-Ion-Beam Scanning Electron Microscope (project no. 386509496) within the Major Research Instrumentation Program.

References
[1] D. Yang, M. Bambach, J. Cao, J. Duflou, P. Groche, T. Kuboki, A. Sterzing, A. Tekkaya, C. Lee, Flexibility in metal forming, CIRP Annals 67 (2018) 743-765. https://doi.org/10.1016/j.cirp.2018.05.004
[2] M.S. Mohebbi, A. Akbarzadeh, Experimental study and FEM analysis of redundant strains in flow forming of tubes, J. Mater. Process. Technol. 210 (2010) 389-395. https://doi.org/10.1016/j.jmatprotec.2009.09.028
[3] B. Arian, M. Riepold, J. Rozo Vasquez, W. Homberg, A. Trächtler, F. Walther, Forming of metastable austenitic stainless steel tubes with axially graded martensite content by flow-forming, ESAFORM 2021, Proceedings of the 24th International Conference on Material Forming, 2021.
[4] M. Runge, Spinning and Flow forming: spinning and flow forming technology, product design, equipment, control systems, Verlag Moderne Industrie, Landsberg/Lech, 1994.
[5] M. Sivanandini, S. Dhami, B. Pabla, Flow forming of tubes: A review, Int. J. Sci. Eng. Res. 3 (2012) 587-597.
[6] M. Riepold, B. Arian, J.V. Rozo, W. Homberg, F. Walther, A. Trächtler, Model approaches for closed-loop property control for flow forming, Adv. Industr. Manuf. Sci. 3 (2021). https://doi.org/10.1016/j.aime.2021.100057
[7] D. Marini, D. Cunningham, P. Xirouchakis, J. Corney, Flow forming: A review of research methodologies, prediction models and their applications, Int. J. Mech. Eng. Technol. 7 (2016) 285-315.
[8] A. Weidner, Deformation processes in TRIP/TWIP steels, Springer International Publishing, Cham, 2020.
[9] N. Gey, B. Petit, M. Humbert, Electron backscattered diffraction study of ε/α martensitic variants induced by plastic deformation in 304 stainless steel, Metall. Mater. Trans. A 36A (2005) 3291-3299. https://doi.org/10.1007/s11661-005-0003-9
[10] P. Haušild, V. Davydov, J. Drahokoupil, M. Landa, P. Pilvin, Characterization of strain-induced martensitic transformation in a metastable austenitic stainless steel, Mater. Des. 31 (2010) 1821-1827. https://doi.org/10.1016/j.matdes.2009.11.008
[11] B. Arian, W. Homberg, L. Kersting, A. Trächtler, J. Rozo Vasquez, F. Walther, Produktkennzeichnung durch lokal definierte Einstellung von ferromagnetischen Eigenschaften

beim Drückwalzen von metastabilen Stahlwerkstoffen, in: 36. Aachener Stahlkolloquium - Umformtechnik „Ideen Form Geben“, 2022, pp.333-347.
[12] T. Angel, Formation of martensite in austenitic stainless steels: Effects of deformation, temperature, and composition, J. Iron Steel Inst. 5 (1954) 165-174.
[13] S.K. Varma, J. Kalyanam, L. Murk, V. Srinivas, Effect of grain size on deformation-induced martensite formation in 304 and 316 stainless steels during room temperature tensile testing, J. Mater. Sci. Lett. 13 (1994) 107-111. https://doi.org/10.1007/BF00416816
[14] J. Biehler, H. Hoche, M. Oechsner, Nitriding behavior and corrosion properties of AISI 304L and 316L austenitic stainless steel with deformation-induced martensite, Surf. Coat. Technol. 324 (2017) 121-128. https://doi.org/10.1016/j.surfcoat.2017.05.059
[15] J. Talonen, P. Aspegren, H. Hänninen, Comparison of different methods for measuring strain induced α-martensite content in austenitic steels, Mater. Sci. Technol. 20 (2004) 1506-1512. https://doi.org/10.1179/026708304X4367
[16] M. Astudillo, M. Nicolás, J. Ruzzante, M. Gómez, G. Ferrari, L. Padovese, M. Pumarega, Correlation between martensitic phase transformation and magnetic Barkhausen noise of AISI 304 steel, Procedia Mater. Sci. 9 (2015) 435-443. https://doi.org/10.1016/j.mspro.2015.05.014